THE GEOLOGICAL SOCIETY OF AMERICA®

Voluminous plutonism during volcanic quiescence revealed by thermochemical modeling of zircon

Casey R. Tierney[1,2], Axel K. Schmitt[3,4], Oscar M. Lovera[3], and Shanaka L. de Silva[1]
[1]College of Earth, Ocean, and Atmospheric Sciences, Oregon State University, Corvallis, Oregon 97331, USA
[2]School of Earth Sciences and Environmental Sustainability, Northern Arizona University, Flagstaff, Arizona 86011, USA
[3]Department of Earth, Planetary, and Space Sciences, University of California–Los Angeles, Los Angeles, California 90095, USA
[4]Institut für Geowissenschaften, Universität Heidelberg, Im Neuenheimer Feld 234-236, 69120 Heidelberg, Germany

ABSTRACT

Five late Pleistocene lava domes with a combined eruptive volume of ~40 km^3 distributed over an area of ~2000 km^2 represent the waning stages of the 10–1 Ma ignimbrite flare-up in the Altiplano Puna Volcanic Complex (APVC) of the Central Andes. Zircon crystal face (on unsectioned rims) and interior (on sectioned crystals) ages (U-Th and U-Pb, respectively) for a total of 252 crystals indicate remarkably consistent zircon crystallization histories: the youngest zircon surface ages (ca. 104–83 ka) are near ^{40}Ar/^{39}Ar eruption ages from sanidine and biotite (ca. 120–87 ka), but a significant population of surface ages predates eruption, ranging to secular equilibrium (with U-Pb interior ages to 3.5 Ma). The essentially continuous zircon crystallization history implies protracted magma presence, which agrees with temporally invariant Ti-in-zircon model temperatures, backed by the homogeneity of indirectly temperature-dependent compositional parameters. Zircon age spectra modeled using a finite-difference thermal and mass-balance model for open-system magma evolution indicate protracted zircon production in the magma reservoirs that require time-integrated recharge rates of ~1 × 10^{-3} km^3/yr, corresponding to high intrusive to extrusive ratios of 75: 1. This rate is below the ~5 × 10^{-3} km^3/yr threshold proposed in the literature for incubating the supereruptions defining the flare-up. When accounting for the shorter durations of high versus low recharge episodes over the ~10 m.y. lifetime of the APVC flare-up, the contributions to composite batholith formation in the shallow crust of the APVC remained broadly constant during peaks and lulls in eruptive activity. This connotes that eruptive fluxes are a poor measure for intrusive fluxes. A corollary of this interpretation is that commonly applied intrusive to extrusive ratios will severely underestimate pluton formation rates during periods of low eruptive flux.

INTRODUCTION

The magma dynamics of cordilleran batholiths and their volcanic equivalents are central to the understanding of growth and stabilization of continental crust, crustal thickening in magmatically active plateaus, geothermal budgets, supereruptions and associated hazards, and economic mineral deposits (e.g., Petford et al., 2000; Bachmann et al., 2007; John, 2008; Caricchi et al., 2014; Lipman and Bachmann, 2015). However, uncertainties about realistic magma fluxes fuel debate on fundamental questions such as whether plutons form rapidly during magmatic flare-ups or more sedately under steady-state magmatism (Ducea, 2001; Glazner et al., 2004; Paterson et al., 2011). Large-volume silicic eruptions are direct evidence for batholith-sized magma accumulations in the shallow (~5–10 km) crust, and they require high recharge rates to keep them eruptible (Annen, 2009; Gelman et al., 2013). Supereruptions as instantaneous events thus require significant build-up times. Model and empirical constraints indicate ~10^6 yr of preeruptive magma residence for individual supereruptions (Wotzlaw et al., 2013); however, magma accumulation times prior to such eruptions collectively only compose 10%–20% of the overall ~10^7 yr duration of flare-up episodes (e.g., de Silva et al., 2015).

Plutonic volumes in batholiths are commonly correlated with erupted volumes (e.g., Smith, 1979; Crisp, 1984). While there is merit to this, there is also the tacit assumption that lulls in volcanism imply lulls in magmatism at depth. Alternatively, eruptive quiescence could merely reflect failure of magma to erupt. To distinguish between these competing scenarios, we use zircon chronochemistry from five discrete but chronologically and magmatically linked lava bodies erupted during late Pleistocene waning of the ignimbrite flare-up of the Altiplano Puna Volcanic Complex (APVC) of the Central Andes. Thermochemical modeling reveals growth of a voluminous pluton in the upper crust of the Central Andes during the late Pleistocene with dimensions that are equivalent to those associated with supereruptions (>500 km^3 magma), although only ~40 km^3 was erupted.

GEOLOGIC BACKGROUND

One of the best-preserved volcanic records of a high-volume magmatic event or flare-up available is that of the APVC of the Central Andes, an extensive ignimbrite plateau where >15,000 km^3 of silicic magma erupted as ignimbrites and lavas from several large calderas and other source structures between ca. 10 and 1 Ma (de Silva et al., 2006; Salisbury et al., 2011). Eruptive activity climaxed in pulses at ca. 8, 6, and 4 Ma; the most recent supereruption, Pastos Grandes, occurred from the eponymous caldera ca. 2.6 Ma (Salisbury et al., 2011). Evidence for an extensive upper crustal batholith underlying the APVC comes from correspondence of the spatiotemporal pattern of volcanism with a large negative Bouguer gravity anomaly and a seismic low-velocity zone extending from 5 to 30 km beneath the surface (Prezzi et al., 2009; Ward et al., 2014), the Altiplano Puna magma body (Chmielowski et al., 1999). Volume estimates for magmatic addition underneath the APVC range over an order of magnitude (~3 × 10^4 to 5 × 10^5 km^3; de Silva and Gosnold, 2007; Ward et al., 2014).

Minor eruptions have continued during the waning stages of the flare-up between 2.6 Ma and present; the most recent phase of APVC volcanism comprises a series of late Pleistocene domes. The five largest of these domes (Chao, Chillahuita, Chanka, Chascon-Runtu Jarita, and Tocopuri; combined erupted lava volume ~40 km^3) are distributed over a roughly elliptical area in an ~75-km-long arc segment centered at 22°S, 68°W (Fig. 1). The best available ^{40}Ar/^{39}Ar eruption ages range between ca. 94 and 87 ka (sanidine for Chascon-Runtu Jarita; see Table DR1 in the GSA Data Repository[1]). Dome lavas strongly resemble one another and the regional ignimbrites in their dacitic to rhyolitic bulk

[1]GSA Data Repository item 2016223, additional analytical methods, modeling details, supplemental figures, Table DR1 (summary of ^{40}Ar/^{39}Ar geochronology), Table DR2 (zircon age and trace element data), and Table DR3 (thermal model parameters), is available online at www.geosociety.org/pubs/ft2016.htm, or on request from editing@geosociety.org.

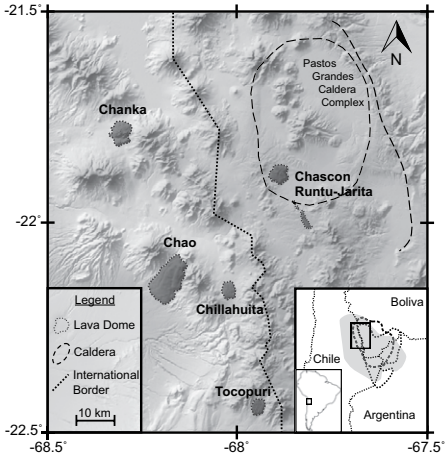

Figure 1. Study area map within the Altiplano Puna Volcanic Complex (APVC), Central Andes. Domes are shaded in dark gray. Inset: regional area showing boundaries of the APVC (shaded gray), the seismically inferred Altiplano-Puna magma body (dashed line), and the negative Bouguer anomaly (dotted line) Prezzi et al., 2009; Ward et al., 2014).

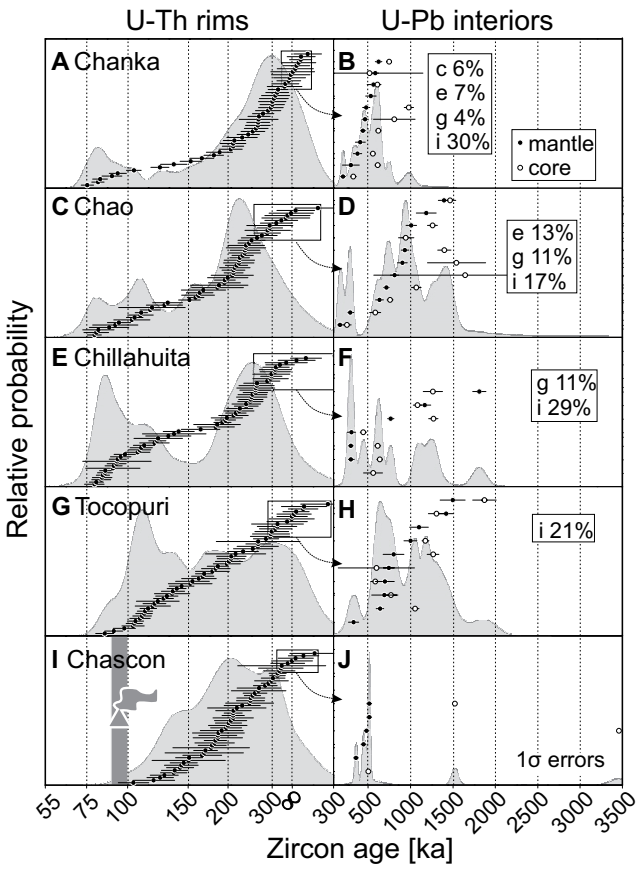

Figure 2. Zircon ages and probability density distributions for individual Altiplano Puna Volcanic Complex (Central Andes) dome lavas plotted with 1σ error bars. Left panels (A, C, E, G, I) show U-Th rim ages for unsectioned zircon crystals with ages on the x-axis calculated as two-point isochron model ages for zircon and melt (i.e., proportional to the logarithm of the isochron slope). Right panels (B, D, F, H, J) are U-Pb ages for mantle and interior pairs for sectioned zircons determined to be in U-Th secular equilibrium (gray boxes). Filled circles represent zircon mantle ages; open circles represent the interior ages. Probability density distributions are indicated by the gray region behind symbols. Boxed percentages indicate the Kolmogorov-Smirnov (KS) probability between the U-Th zircon rim ages for an individual dome lava compared to other samples as identified by the panel letter.

composition, mineralogical and isotopic characteristics, hydrous mafic mineralogy (hornblende and biotite), and occasional andesitic inclusions (de Silva et al., 1994; Watts et al., 1999; Salisbury et al., 2011). They differ from the ignimbrites only by higher textural maturity (centimeter-sized phenocrysts at ~50% crystallinity; de Silva et al., 1994; Watts et al., 1999).

ZIRCON GEOCHRONOLOGY AND GEOCHEMISTRY

Zircon surfaces (by U-Th on unsectioned crystals) as well as mantle and interiors of secular equilibrium zircons (by U-Pb after sectioning crystals) were dated for a total of 252 crystals subequally distributed over all 5 domes (Table DR2). An ~50% subset of age-representative crystals were also analyzed for trace element [Ti, Y + REE (rare earth element), Hf] abundances in the same analysis spot used for dating (Table DR2; Figs. DR1–DR5). Trace element characteristics of the zircons confirm equilibrium with their highly crystalline host lavas (Fig. DR2), which equilibrated at comparatively shallow depths (<10 km) (de Silva et al., 1994; de Silva and Gosnold, 2007). Although Ti-in-zircon (Ferry and Watson, 2007) correlates with indirectly temperature (*T*) dependent compositional parameters (e.g., Zr/Hf; Fig. DR3), it is difficult to quantify absolute temperatures, and we thus parsimoniously interpret the invariance of Ti-in-zircon and Zr/Hf as an indication of the general similarity between samples, and as being permissive for minimal ($<10^{-4}$ °C/yr) secular cooling over time scales of >500 k.y. (Fig. DR4).

The youngest zircon surface age populations (ca. 83, 85, and 89 ka for Chanka, Chillahuita, and Chao; ca. 101 and 104 ka for Tocopuri and Chascon-Runtu Jarita, respectively) are close to the eruption ages, but in all samples a significant, and often dominant, population of zircon surface ages predate the eruption, ranging to secular equilibrium (ca. 350 ka; Fig. 2). U-Pb mantle and interior ages form discrete peaks consisting of individual or clusters of few analyses ranging to ca. 1 Ma, and for a single zircon interior from Chascon, to 3.5 Ma (Fig. 2).

Kolmogorov-Smirnov (KS) (Press et al., 1988) statistical analysis is used to further quantify the similarity in the zircon age populations between the domes. When comparing the zircon crystal surface ages between the domes, acceptable KS probabilities P = 11%–29% are obtained; typically P <5% is the threshold to reject the null hypothesis that the samples are drawn from the same distribution at the 95% level of confidence (Fletcher et al., 2007). The lone exception is the dome pair (Chanka and Tocopuri; P = 4%), which shows a slightly lower level of similarity, possibly because these domes represent the northernmost and southernmost end members of the late Pleistocene APVC domes. The overall zircon age concordance between domes and their chemical similarities indicates a coherent magmatic and thermal history in an extensive (~2000 km^2) crustal segment with the footprint of a large caldera.

THERMOCHEMICAL MODELING

Conductive heat transport models provide first-order constraints on magma volumes and rates of recharge required to maintain the environment conducive for zircon crystallization (Caricchi et al., 2014). To quantify the recharge rate (i.e., input rate into a seed magma chamber) required to generate the observed zircon age distribution, we have developed the first finite-difference thermal and mass-balance model for open-system magma evolution (recharge-assimilation-fractional crystallization; RAFC), where zircon crystallization is treated in accord with experimentally constrained zircon saturation (Table DR3; Figs. DR6–DR8).

Model Specifics

A two-dimensional thermal diffusion model with temperature-dependent diffusivity-conductivity (Whittington et al., 2009) and incorporating the effects of magma RAFC was developed using a finite difference discretization by the alternating-direction implicit method. All calculations were run on a grid of 20 × 60 km (width × depth), and cell sizes of 0.1 × 0.1 km. The model implements an experimentally constrained nonlinear crystallization curve for intermediate magmas (modified from Harrison et al., 2007) and a typical temperature-assimilation relationship obtained from Spera and Bohrson (2001). Sensitivity tests agree well with published conductive cooling models (Gelman et al., 2013; Caricchi et al., 2014). The recharge magma temperature was 1000 °C, in agreement with thermometry for mafic lavas in the Chascon-Runtu Jarita complex

(Watts et al., 1999). An initial geothermal gradient of ~50 °C/km was imposed as the background thermal state of the instantaneous ellipsoidal magma intrusion of ~50 km^3 emplaced at 7 km depth, consistent with the thermobarometry of the APVC domes. In contrast to previous models (Caricchi et al., 2014), zircon generated in each cell was quantified taking into account the thermal and compositional dependence of zircon saturation (Boehnke et al., 2013). Periodic instantaneous episodes of recharge at the center of the chamber are simulated, followed by radial outward growth of the magma chamber following the mass conservation law. A more protracted build-up extends the duration of zircon crystallization, but does not significantly alter the relative abundances of newly formed versus recycled zircons. Similarly, changing intrusion geometry or timing (in the current model every 5 k.y.) yields qualitatively similar zircon crystallization patterns. Input parameters for the model are summarized in the Data Repository.

Model Recharge Rates and Plutonic Volumes

Modeling results (Fig. 3) predict that zircon produced in an intrusion built up at low recharge rates (<1 × 10^{-3} km^3/yr) will not match the observed age distribution and will instead be dominated by zircon antecrysts (i.e., the percentage of zircons crystallized within >250 k.y. before the eruption would be >98% of the total for a model run duration of 500 k.y.; Fig. 3). By contrast, model peak flare-up recharge rates (>1 × 10^{-2} km^3/yr; de Silva and Gosnold, 2007) would result in excessive volumes of zircon-undersaturated magma that upon cooling would produce zircon during a comparatively brief (~100 k.y.) spike, which is also at odds with the observed age distribution. A recharge rate of >1 × 10^{-3} km^3/yr is required to match the steady-state cumulative probability curves for the samples (Fig. 3; all domes). At recharge rates >5 × 10^{-3} km^3/yr, the physical state of the intrusive reservoir is also predicted to differ dramatically from that formed at lower rates; at ~1–3 × 10^{-3} km^3/yr, the amount of eruptible magma only marginally increases compared to the initial conditions, whereas it reaches supereruption proportions (500 km^3 of magma) at >5 × 10^{-3} km^3/yr after 500 k.y. (Gelman et al., 2013).

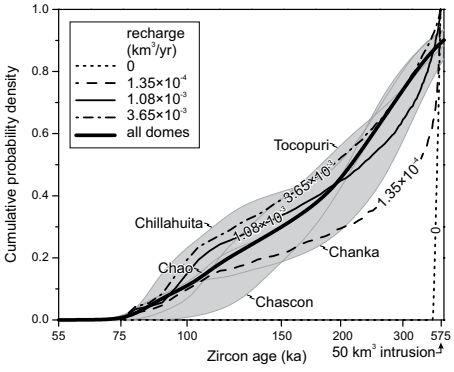

Figure 3. Cumulative probability curves for individual (thin gray lines) and all Altiplano Puna Volcanic Complex (Central Andes) dome lavas (thick black line) with model zircon crystallization age spectra showing the amount of zircon crystallizing during a 500 k.y. interval starting with the initial emplacement of a 50 km^3 intrusion, and ending with a model eruption age of 75 ka. Model curves are calculated for 4 different recharge rates between 0 and 3.65 × 10^{-3} km^3/yr; higher rates (not shown) would lead to rapid growth of magma above zircon saturation, limiting the preservation potential of early-crystallized zircon. See caption of Figure 2 for an explanation of the x-axis scale.

Existing thermal models fall short of tracking pathways of individual magma parcels and their zircon cargo, but we reasonably assume that zircons generated over protracted time periods are well mixed because compositional homogeneity is readily achieved by convection and overturn in silicic magmas (Huber et al., 2009). There is potential for missing early crystallization events in our data (e.g., if some older zircons were locked away in the solidified margins of the intrusions; Shane et al., 2012), but this would only affect our assessment of the longevity of the system, not of the required recharge rate that can protractedly and continuously produce zircon without becoming overwhelmed by antecrysts.

Consequently, combining the initial intrusion with accumulated volumes from subsequent best-fit recharge at >1 but <5 × 10^{-3} km^3/yr, the model results require that at least 600 km^3 of mushy intrusions underpin each of the 5 domes by the time of eruption, and for adjacent domes these subvolcanic plutons likely start to merge. The APVC domes are the only mapped late Pleistocene eruptions in this segment of the APVC, and excellent preservation of volcanic units under arid conditions precludes that contemporaneous eruptions have been missed or eroded. The combined volume of >3000 km^3 for the plutonic underpinnings of the APVC domes dwarfs the total erupted volume of ~40 km^3. Using the best-fit model recharge rates results in an intrusive to extrusive ratio of >75:1, which greatly exceeds commonly cited estimates of ~10:1 (Smith, 1979; Crisp, 1984) for caldera-related magmatic systems and even the geophysically constrained ratios of 20–35:1 for the duration of the APVC flare-up (Ward et al., 2014), and may reflect the highly crystalline condition of a magma mush preventing eruption under steady-state conditions.

To estimate the relative contributions of magmatic addition during volcanic peaks versus lulls over the entire ~10 m.y. duration of the APVC flare-up, we calculated the magmatic addition of 1–2 caldera-forming eruptions per arc segment with individual lifetimes of 1 m.y. forming at high recharge rates of 5 × 10^{-3} km^3/yr (Gelman et al., 2013). For the remaining duration of the flare-up, we conservatively apply the lower bound of recharge rates modeled from zircon age spectra of late Pleistocene APVC domes (1 × 10^{-3} km^3/yr) (intrusive volumes for peak = 1 m.y. × 5 × 10^{-3} km^3/yr; lull = 9 m.y. × 1 × 10^{-3} km^3/yr; volume peak divided by lull = 0.56; alternatively: peak = 2 m.y. × 5 × 10^{-3} km^3/yr; lull = 8 m.y. × 1 × 10^{-3} km^3/yr; peak:lull = 1.25. For 75 km arc length and a 10 m.y. duration, total intrusive addition at these rates equals 19 and 24 km^3/m.y./km arc; this translates into 1.0 to 1.2 Armstrong units, i.e., km^3/yr for Earth's 51,000 km of convergent margins). This simple (ignoring erupted volumes) mass balance indicates that the composite batholith underneath the APVC consists of roughly subequal proportions of plutonic remnants of supereruptions (eruptive peaks) and intrusions related to eruptive lulls or waning periods.

This work bridges alternate viewpoints that debate the relative roles of high versus low fluxes in cordilleran batholith formation. Eruptive activity is not a comprehensive proxy for plutonic activity, and zircon longevity for APVC lavas suggests that shallow magma accumulation rates based on inversion of erupted volumes are significantly underestimated, with obvious implications for any propagation of these to deeper magma production rates. The correlation of eruptive vigor with recharge rates confirms the positive feedbacks between magma intrusion, eruptible magma incubation, and thermomechanics of the upper crust. During eruptive lulls, lower recharge rates promote long-term storage over eruption, while high recharge rates promote unsustainable growth of large magma bodies that eventual erupt catastrophically (Gregg et al., 2012; de Silva and Gregg, 2014), although the relative volume of plutonic remnants may be subequal.

CONCLUSIONS

Zircon data for APVC domes, when interpreted through a thermochemical model, call for the presence of sizable thermally and materially connected plutons that are concealed underneath a ~2000 km^2 area along the western margin of the APVC, well within the bounds of the suspected APVC batholith. This model suggests that during flare-up, when rates of recharge were approximately 5× higher (e.g., Gelman et al., 2013), individual intrusions would become integrated and homogenized, and significant volumes of eruptible magma would form. However, as the recharge rate waned during the Pleistocene, and by analogy during periods between supervolcanic episodes, incubation of discrete magma inputs became less efficient, limiting the merging of individual eruptible magma volumes and retarding thermal softening of the roof of the intrusive complex (e.g., Gregg et al., 2012). Thus, although cumulative intrusive volumes of supereruption proportions are predicted beneath

the domes, cataclysmic eruption was prevented. These domes thus represent a rare window into pluton assembly during low eruptive flux stages of a magmatic flare-up and reveal the incremental construction of the most recent part of the APVC batholith, which is the product of extensive accumulation of individual intrusions ranging in scale over several orders of magnitude (de Silva and Gosnold, 2007; de Silva et al., 2015). In consequence, eruptive flux is not necessarily a proxy for intrusive flux at depth, and significant plutonic volumes can develop during the lulls and waning stages of magmatic flare-ups. Although the modeled recharge rates are strictly only applicable to the APVC, there are broader implications in that pluton formation during eruptive lulls has been largely ignored in quantifying arc crustal growth in general.

ACKNOWLEDGMENTS

We thank George Bergantz, Mihai Ducea, Oliver Jagoutz, Calvin Miller, Juan Otamendi, and an anonymous reviewer for their thoughtful comments. This work was made possible by National Science Foundation grants EAR-0838536 and EAR-1029193. The ion microprobe facility at the University of California–Los Angeles is partly supported by a grant from the Instrumentation and Facilities Program, Division of Earth Sciences, National Science Foundation.

REFERENCES CITED

Annen, C., 2009, From plutons to magma chambers: Thermal constraints on the accumulation of eruptible silicic magma in the upper crust: Earth and Planetary Science Letters, v. 284, p. 409–416, doi:10.1016/j.epsl.2009.05.006.

Bachmann, O., Miller, C.F., and de Silva, S.L., 2007, The volcanic-plutonic connection as a stage for understanding crustal magmatism: Journal of Volcanology and Geothermal Research, v. 167, p. 1–23, doi:10.1016/j.jvolgeores.2007.08.002.

Boehnke, P., Watson, E.B., Trail, D., Harrison, T.M., and Schmitt, A.K., 2013, Zircon saturation re-revisited: Chemical Geology, v. 351, p. 324–334, doi:10.1016/j.chemgeo.2013.05.028.

Caricchi, L., Simpson, G., and Schaltegger, U., 2014, Zircons reveal magma fluxes in the Earth's crust: Nature, v. 511, p. 457–461, doi:10.1038/nature13532.

Chmielowski, J., Zandt, G., and Haberland, C., 1999, The Central Andean Altiplano-Puna magma body: Geophysical Research Letters, v. 26, p. 783–786, doi:10.1029/1999GL900078.

Crisp, J.A., 1984, Rates of magma emplacement and volcanic output: Journal of Volcanology and Geothermal Research, v. 20, p. 177–211, doi:10.1016/0377-0273(84)90039-8.

de Silva, S.L., and Gosnold, W.D., 2007, Episodic construction of batholiths: Insights from the spatiotemporal development of an ignimbrite flare-up: Journal of Volcanology and Geothermal Research, v. 167, p. 320–335, doi:10.1016/j.jvolgeores.2007.07.015.

de Silva, S.L., and Gregg, P.M., 2014, Thermomechanical feedbacks in magmatic systems: Implications for growth, longevity, and evolution of large caldera-forming magma reservoirs and their supereruptions: Journal of Volcanology and Geothermal Research, v. 282, p. 77–91, doi:10.1016/j.jvolgeores.2014.06.001.

de Silva, S.L., Self, S., Francis, P.W., Drake, R.E., and Ramirez, R.C., 1994, Effusive silicic volcanism in the Central Andes: The Chao dacite and other young lavas of the Altiplano-Puna Volcanic Complex: Journal of Geophysical Research, v. 99, p. 17,805–17,825, doi:10.1029/94JB00652.

de Silva, S.L., Zandt, G., Trumbull, R., and Viramonte, J., 2006, Large scale silicic volcanism: The result of thermal maturation of the crust, *in* Chen Yun-tai, ed., Advances in geosciences: Proceedings of the Asia-Oceania Geosciences Society: River Edge, New Jersey, World Scientific Press, p. 215–230.

de Silva, S.L., Riggs, N.R., and Barth, A.P., 2015, Quickening the pulse: Fractal tempos in continental arc magmatism: Elements, v. 11, p. 113–118, doi:10.2113/gselements.11.2.113.

Ducea, M., 2001, The California Arc: Think granitic batholiths, eclogitic residues, lithospheric-scale thrusting, and magmatic flare-ups: GSA Today, v. 11, p. 4–10, doi:10.1130/1052-5173(2001)011<0004:TCATGB>2.0.CO;2.

Ferry, J.M., and Watson, E.B., 2007, New thermodynamic models and revised calibrations for the Ti-in-zircon and Zr-in-rutile thermometers: Contributions to Mineralogy and Petrology, v. 154, p. 429–437, doi:10.1007/s00410-007-0201-0.

Fletcher, J.M., Grove, M., Kimbrough, D., Lovera, O., and Gehrels, G.E., 2007, Ridge-trench interactions and the Neogene tectonic evolution of the Magdalena shelf and southern Gulf of California: Insights from detrital zircon U-Pb ages from the Magdalena fan and adjacent areas: Geological Society of America Bulletin, v. 119, p. 1313–1336, doi:10.1130/B26067.1.

Gelman, S.E., Gutierrez, F.J., and Bachmann, O., 2013, On the longevity of large upper crustal silicic magma reservoirs: Geology, v. 41, p. 759–762, doi:10.1130/G34241.1.

Glazner, A.F., Bartley, J.M., Coleman, D.S., Gray, W., and Taylor, R.Z., 2004, Are plutons assembled over millions of years by amalgamation from small magma chambers?: GSA Today, v. 14, p. 4–11, doi:10.1130/1052-5173(2004)014<0004:APAOMO>2.0.CO;2.

Gregg, P.M., de Silva, S.L., Grosfils, E.B., and Parmigiani, J.P., 2012, Catastrophic caldera-forming eruptions: Thermomechanics and implications for eruption triggering and maximum caldera dimensions on Earth: Journal of Volcanology and Geothermal Research, v. 241–242, p. 1–12, doi:10.1016/j.jvolgeores.2012.06.009.

Harrison, T.M., Watson, E.B., and Aikman, A.B., 2007, Temperature spectra of zircon crystallization in plutonic rocks: Geology, v. 35, p. 635–638, doi:10.1130/G23505A.1.

Huber, C., Bachmann, O., and Manga, M., 2009, Homogenization processes in silicic magma chambers by stirring and mushification (latent heat buffering): Earth and Planetary Science Letters, v. 283, p. 38–47, doi:10.1016/j.epsl.2009.03.029.

John, D.A., 2008, Supervolcanoes and metallic ore deposits: Elements, v. 4, p. 22, doi:10.2113/GSELEMENTS.4.1.22.

Lipman, P.W., and Bachmann, O., 2015, Ignimbrites to batholiths: Integrating perspectives from geological, geophysical, and geochronological data: Geosphere, v. 11, p. 705–743, doi:10.1130/GES01091.1.

Paterson, S.R., Okaya, D., Memeti, V., Economos, R., and Miller, R.B., 2011, Magma addition and flux calculations of incrementally constructed magma chambers in continental margin arcs: Combined field, geochronologic, and thermal modeling studies: Geosphere, v. 7, p. 1439–1468, doi:10.1130/GES00696.1.

Petford, N., Cruden, A.R., McCaffrey, K.J.W., and Vigneresse, J.-L., 2000, Granite magma formation, transport and emplacement in the Earth's crust: Nature, v. 408, p. 669–673, doi:10.1038/35047000.

Press, W.H., Flannery, B.P., Teukolsky, S., and Vetterling, W.T., 1988, Numerical recipes in C: The art of scientific computing: Cambridge, UK, Cambridge University Press, 1018 p.

Prezzi, C.B., Götze, H.-J., and Schmidt, S., 2009, 3D density model of the Central Andes: Physics of the Earth and Planetary Interiors, v. 177, p. 217–234, doi:10.1016/j.pepi.2009.09.004.

Salisbury, M.J., Jicha, B.R., de Silva, S.L., Singer, B.S., Jimenez, N.C., and Ort, M.H., 2011, $^{40}Ar/^{39}Ar$ chronostratigraphy of Altiplano-Puna volcanic complex ignimbrites reveals the development of a major magmatic province: Geological Society of America Bulletin, v. 123, p. 821–840, doi:10.1130/B30280.1.

Shane, P., Storm, S., Schmitt, A.K., and Lindsay, J.M., 2012, Timing and conditions of formation of granitoid clasts erupted in recent pyroclastic deposits from Tarawera Volcano (New Zealand): Lithos, v. 140–141, p. 1–10, doi:10.1016/j.lithos.2012.01.012.

Smith, R.L., 1979, Ash-flow magmatism, *in* Chapin, C.E., and Elston, W.E., eds., Ash-flow tuffs: Geological Society of America Special Paper 180, p. 5–28, doi:10.1130/SPE180-p5.

Spera, F.J., and Bohrson, W.A., 2001, Energy-constrained open-system magmatic processes I: General model and energy-constrained assimilation and fractional crystallization (EC-AFC) formulation: Journal of Petrology, v. 42, p. 999–1018, doi:10.1093/petrology/42.5.999.

Ward, K.M., Zandt, G., Beck, S.L., Christensen, D.H., and McFarlin, H., 2014, Seismic imaging of the magmatic underpinnings beneath the Altiplano-Puna volcanic complex from the joint inversion of surface wave dispersion and receiver functions: Earth and Planetary Science Letters, v. 404, p. 43–53, doi:10.1016/j.epsl.2014.07.022.

Watts, R.B., de Silva, S.L., de Rios, G.J., and Croudace, I., 1999, Effusive eruption of viscous silicic magma triggered and driven by recharge: A case study of the Cerro Chascon-Runtu Jarita Dome Complex in southwest Bolivia: Bulletin of Volcanology, v. 61, p. 241–264, doi:10.1007/s004450050274.

Whittington, A.G., Hofmeister, A.M., and Nabelek, P.I., 2009, Temperature-dependent thermal diffusivity of the Earth's crust and implications for magmatism: Nature, v. 458, p. 319–321, doi:10.1038/nature07818.

Wotzlaw, J.-F., Schaltegger, U., Frick, D.A., Dungan, M.A., Gerdes, A., and Gunther, D., 2013, Tracking the evolution of large-volume silicic magma reservoirs from assembly to supereruption: Geology, v. 41, p. 867–870, doi:10.1130/G34366.1.

Manuscript received 7 April 2016
Revised manuscript received 21 June 2016
Manuscript accepted 21 June 2016

Printed in USA